JOURNAL OF MATERIALS SCIENCE 25 (1990) 2949–2957

High-resolution interface analysis of SiC-whisker-reinforced Si_3N_4 and Al_2O_3 ceramic matrix composites

W. BRAUE*, R. W. CARPENTER, D. J. SMITH‡
Center for Solid State Science, Arizona State University, Tempe, Arizona 85287–1704, USA

Whisker/matrix interfaces between β-SiC whiskers and β-Si_3N_4 or α-Al_2O_3 matrices in composites were examined by high-resolution electron microscopy (HREM), and electron energy loss (ELS) and energy dispersive X-ray (EDS) spectroscopies. Most whisker/matrix interfaces were crystalline, with whiskers directly bonded to matrix crystals. Some whisker/matrix interface regions contained amorphous thin films and these occurred more often in the Si_3N_4 composite, which contained sintering additives, than in the Al_2O_3 matrix composite, which did not. No evidence for light element segregation at crystalline whisker/matrix interfaces was detected by ELS or EDS at 5 nm spatial resolution. Impurities were concentrated in glassy regions in matrix grain boundaries, triple junctions, or at infrequent whisker/matrix interfaces containing amorphous films.

1. Introduction

Whisker reinforcement offers an effective toughening concept for monolithic structural ceramics. In particular, SiC whiskers combine high strength and high elastic moduli with good thermal stability, and are compatible with most oxide and non-oxide matrices. For SiC-whisker-toughened Al_2O_3 a considerable improvement in fracture toughness compared to the matrix material ($\sim 3\,MPa\,m^{-1/2}$) has been achieved. Wei and Becher [1] give a value of $9\,MPa\,m^{-1/2}$ for a 20 vol % SiC whisker/Al_2O_3 composite at room temperature. Bending strength was also found to increase. Similar, although less pronounced, effects of whisker reinforcement on mechanical properties of Si_3N_4 have been reported [2, 3]. Crack branching, crack deflection and crack bridging have been identified as the major toughening mechanisms in SiC-whisker-reinforced Al_2O_3 and Si_3N_4 [4].

Besides residual stresses in the composite due to differences in thermal expansion and elastic properties of both constituents, toughening mechanisms depend critically on interfacial properties of the composite. Contrary to fibre reinforcement, little if any pull-out of the toughening component is evident in whisker-toughened ceramics [5]. Dynamic *in situ* straining experiments performed recently in a high-voltage electron microscope confirmed that interfacial debonding was a prerequisite for effective whisker toughening, as required by composite fracture mechanics [6]. Qualitatively, a 'weak' interface, possibly involving amorphous interlayers, may be more likely to debond under stress than a 'strong' interface between SiC whiskers and the surrounding matrix.

Evaluation of the chemical and geometric structure of an interface on a subnanometre scale requires the combined capabilities of both high-resolution electron microscopy (HREM) and small-probe microanalysis (EDS and ELS). This is especially true when amorphous phases are present at the interface. This combined approach was applied to 20 vol % SiC-whisker-reinforced Al_2O_3 and Si_3N_4 matrix ceramic composites, to evaluate the structural and chemical characteristics of interfaces between crystalline whiskers and matrices.

2. Experimental procedures

2.1. Materials

The Al_2O_3 base composite was hot-pressed at 1830° C, 60 MPa, in a vacuum without sintering aid or organic/precursor additions. The Si_3N_4 base material was hot-pressed at 1725° C, 30 MPa, in 1 bar argon atmosphere, with 6 wt % (Y_2O_3 + Al_2O_3) added to promote densification. Both materials were reinforced with 20 vol. % β-SiC whiskers from Tokai Carbon Ltd, Japan (Tokamax).

The Al_2O_3 matrix was prepared from Reynolds RC–HP DBM powder with MgO (0.03 wt %) and SiO_2 (0.02 wt %) being the major impurities. Toyo Soda TS7 α-Si_3N_4 powder was employed for the Si_3N_4 matrix with the major impurities being oxygen (1.4 wt %), and the sum of aluminium, iron, calcium and magnesium being equal to 0.01 wt %, and 0.1 wt % chlorine. Major bulk impurities in as-received β-SiC Tokamax whiskers were analysed by standard chemical methods, and compared with similar VLS-grown whisker materials from different sources, for example,

* *Permanent address*: German Aerospace Research Establishment (DFVLR), Materials Research Institute, D-5000 Cologne 90, FRG.
‡ Also at Department of Physics.

0022–2461/90 $03.00 + .12

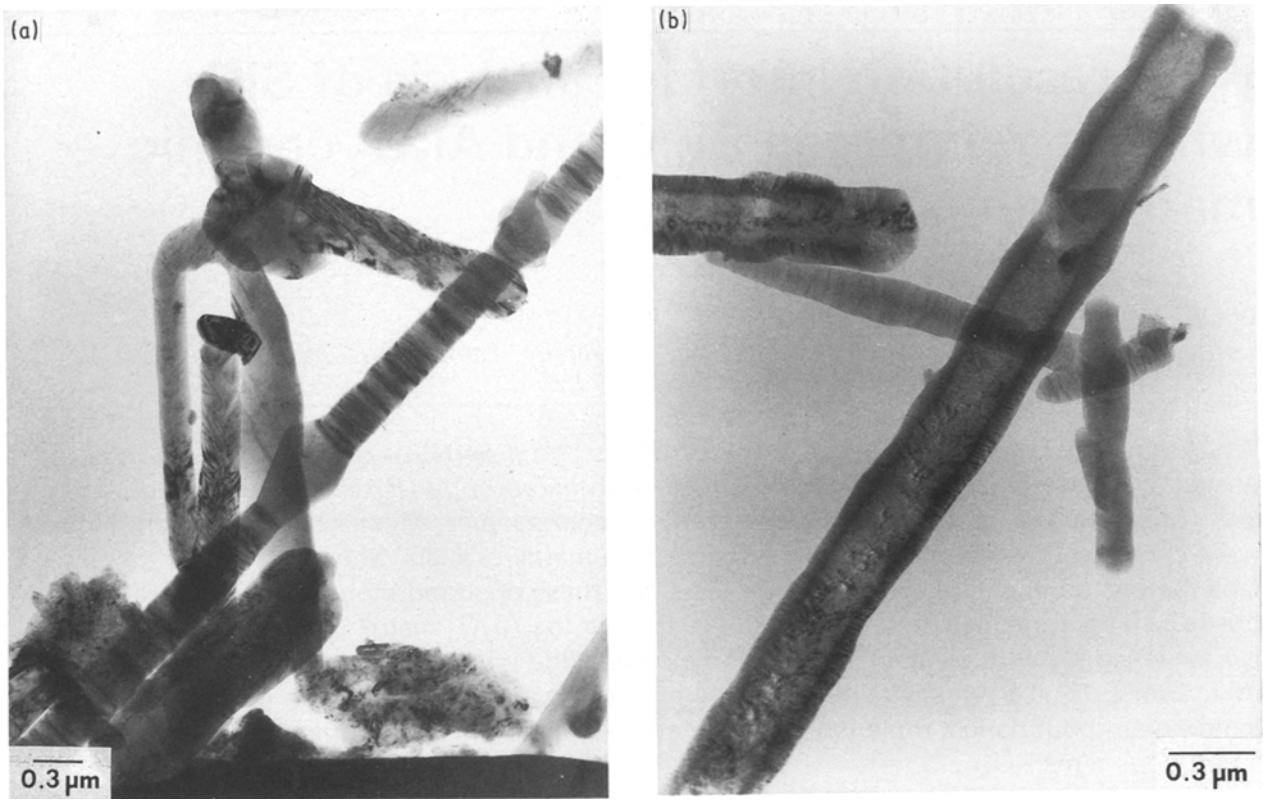

Figure 1 Bright field (BF) images of as-received β-SiC whiskers from Tokai Carbon Ltd (a) and Tateho Chemical Industries (b) at 300 kV, from [7].

Tateho Chemical Industries, Japan (see Fig. 1). Both lots contained considerable amounts of oxygen, nitrogen and excess carbon, and the Tateho whiskers also contained a substantial amount of calcium. (Tokamax: carbon, 29.27 wt %; nitrogen 0.70 wt %; oxygen, 0.2 wt %; silicon, 69.6 wt %; calcium, 0.01 wt %. Tateho: carbon, 28.53 wt %; nitrogen, 1.37 wt %; oxygen, 1.04 wt %; silicon, 68.0 wt %; calcium, 0.52 wt % [7]. Usually, β-SiC whiskers contain a large variety of additional impurities such as magnesium, aluminium and iron, with one or the other deliberately added in order to increase yield during whisker synthesis. The Tateho whiskers had a total metallic impurity content of about 0.6 wt %, primarily copper, magnesium and aluminium. The total metallic impurity content of the Tokai whiskers was less, about 0.3 wt %, but consisted of a larger number of metals, the principal ones being iron, sodium, aluminium, potassium, chromium, titanium and nickel. These total metallic impurity contents are between the extreme values given for Los Alamos and Silag β-SiC whiskers [8]. Surface-analytical methods (AES, XPS) revealed an enrichment of light elements at the whisker surfaces, which in the case of oxygen was typically an order of magnitude higher than the bulk (see also Section 3.).

2.2. Instrumentation

HREM images from β-SiC/Al_2O_3 and β-SiC/β-Si_3N_4 boundaries were taken in a JEM-4000EX at 400 kV. A Philips EM400 TEM/STEM fitted with a field emission gun operated at 100 kV was used for microanalytical work. ELS spectra were collected with a Gatan serial spectrometer using a sensitivity of 1 eV per channel and approximately equal beam convergence and acceptance half angles (10 mrad). A 5 nm TEM probe was typically used during acquisition ELS and EDS spectra. A low-drift, double-tilt nitrogen cold stage was employed to eliminate specimen contamination during small probe microanalysis and microdiffraction.

Thin foils of the composites were prepared by dimpling and subsequent ion-beam thinning. Orientation of the foils was normal to the hot-pressing axis. As-received SiC whiskers were found to be sufficiently transparent to the electron beam for conventional diffraction contrast transmission electron microscopy.

3. Results

To evaluate possible influences of the whisker surface characteristics on the interfacial structure of these composites, as-received whiskers were studied in more detail by TEM (Fig. 1). They showed fluctuations in aspect ratio and considerable planar disorder perpendicular to the $<1\,1\,1>$ growth axis, indicated by the typical contrast bands in the bright field (BF) images of Fig. 1 or intensive streaking in the corresponding electron diffraction patterns (see also Fig. 6). Minor amounts of agglomerated SiC particulates were attached to whiskers of both brands. Tateho whiskers showed low-density core regions which are typical for rice-hull-derived, VLS-grown SiC whiskers [9]. The morphological integrity of the β-SiC whiskers, as shown in Fig. 2, is not well preserved during powder processing of the composites. Less severe processing techniques such as slip casting, are necessary to minimize whisker damage during composite synthesis.

The general microstructure of the two composites

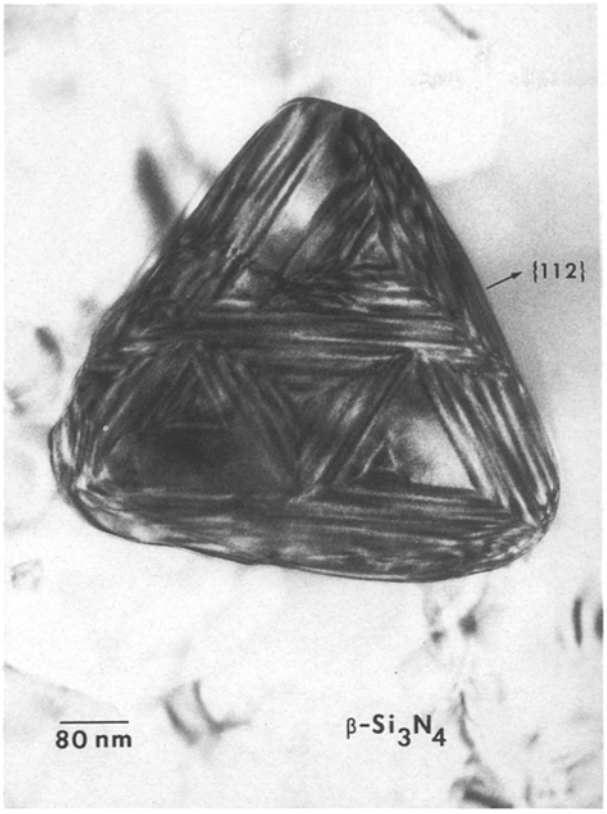

Figure 2 Idiomorphic β-SiC whisker in powder-processed Si_3N_4 base composite revealing {1 1 2} planes (Tokai Carbon Ltd). Orientation is parallel to [1 1 1].

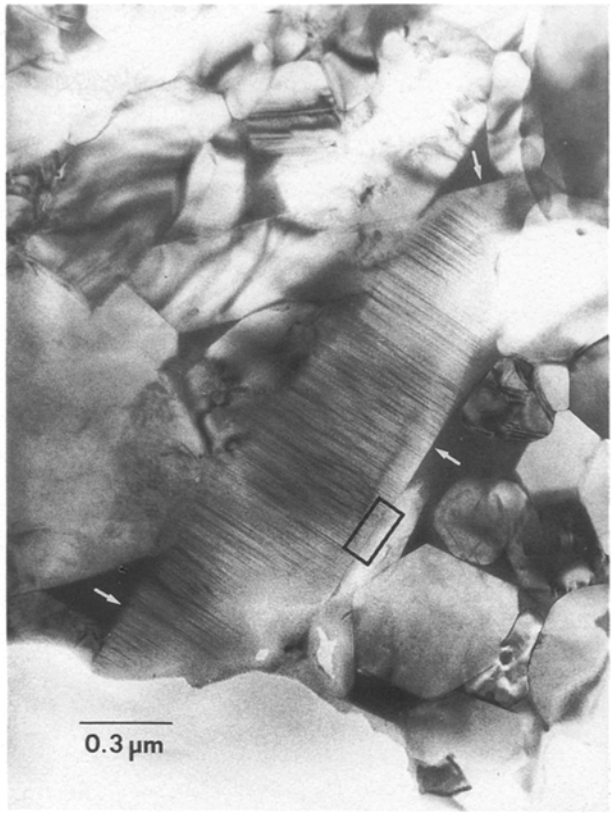

Figure 3 BF image of 20 vol % SiC/Si_3N_4 composite doped with Y_2O_3 and Al_2O_3. Arrows indicate areas of whisker surfaces adjacent to non-crystalline phase. Boxed area was established as suitable location for imaging β-SiC/β-Si_3N_4 boundaries (see text and Fig. 8).

is displayed in the low-magnification BF images of Figs 3, 4 and 5. The Si_3N_4 material consisted of fully transformed β-type Si_3N_4, an yttrium- and aluminium-bearing non-crystalline phase and minor amounts of an yttrium- and aluminium-bearing crystalline silicon oxynitride, which was presumably the same as the J-phase $Y_4Si_2O_7N_2$ identified earlier [10]. Typical grain size of the β-Si_3N_4 matrix was about 2 μm. The matrix of the Al_2O_3 base composite was almost 100% corundum, with very minor amounts of glassy phase. Because densification of Al_2O_3 does not necessarily require the addition of sintering additives, and none were added here, the amount of glassy phase is approximately an order of magnitude lower than for the corresponding Si_3N_4 matrix composite.

The surface morphology of the β-SiC whiskers is related to internal structural characteristics and makes an important contribution to whisker/matrix interactions in all-ceramic composites. Fig. 6 is a BF image of a Tokamax SiC whisker from the Si_3N_4 matrix composite. The tiny band adjacent to the edge of the

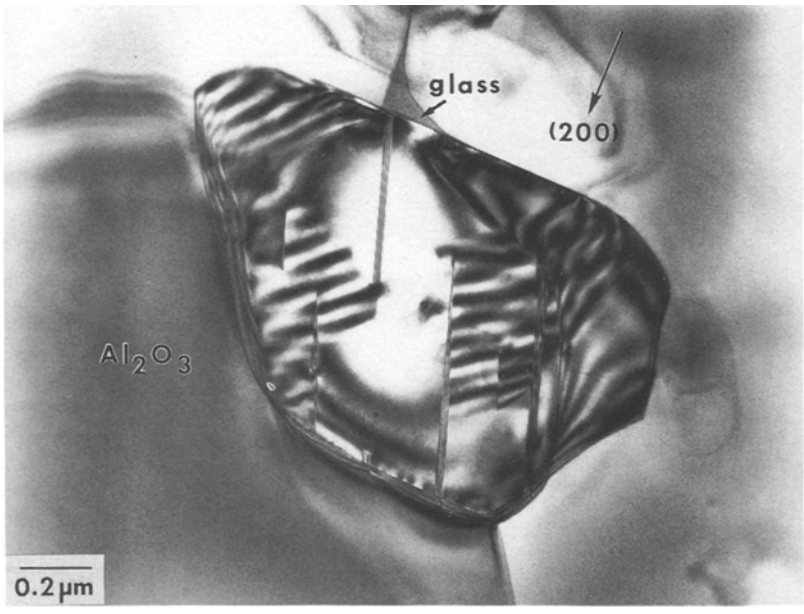

Figure 4 Low magnification BF image of Al_2O_3-based composite revealing small, amorphous triple junction adjacent to β-SiC whisker.

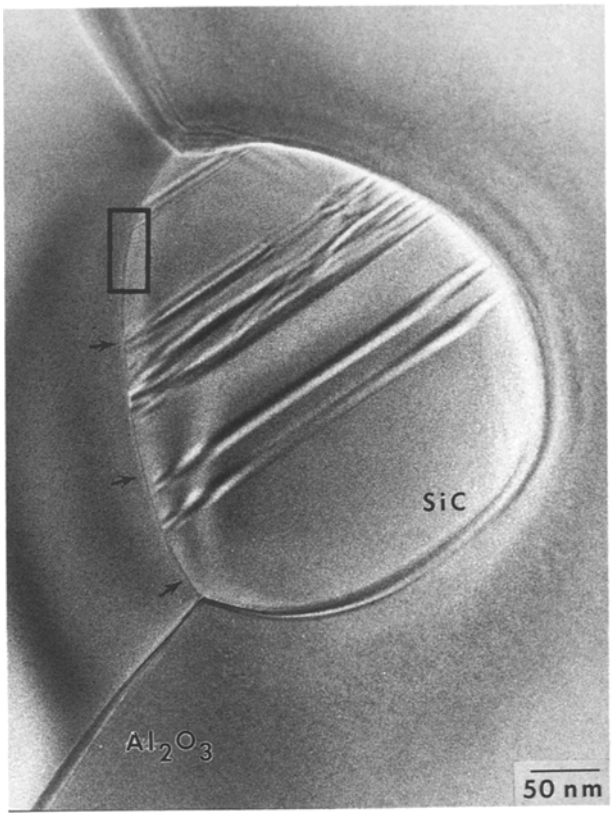

Figure 5 Low-magnification BF image of β-SiC/corundum contact selected for HREM interface imaging (see Fig. 9).

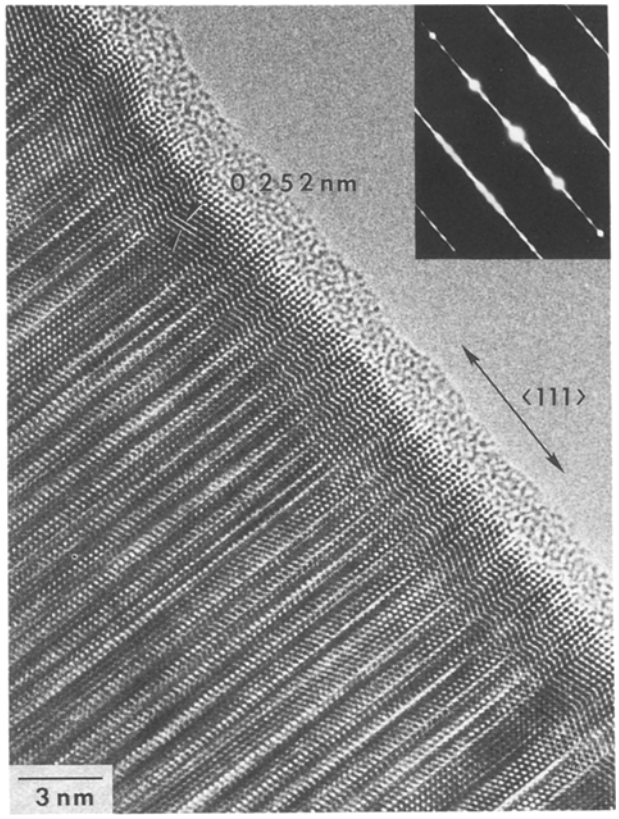

Figure 6 HREM image (400 kV) of β-SiC whisker (Tokai Carbon Ltd) from Si_3N_4 base composite. Beam direction parallel to [1 1 0]. Note that whisker is close to the edge of the foil, amorphous phase contrast is due to ion-beam thinning of the specimen.

foil displaying amorphous phase contrast results from radiation damage during ion-beam thinning of the composite, and is not an intrinsic feature of the as-received whisker surface. This effect occurs in similar images from either composite. The [1 1 0] orientation of this whisker revealed the high concentration of planar faults which gave rise to intensive streaking in the corresponding electron-diffraction pattern (see Fig. 6, inset). Because of this unidimensional disorder perpendicular to the growth axis it is impossible to assign a single well-defined polytype to the whisker. The structural configuration of the whisker is best described as a random mixture of short-period SiC polytypes, as emphasized in the literature [11, 12]. The whisker surface actually consisted of tiny microfacets of alternating {1 1 1} planes, as implied by the very thin areas of Fig. 6. The stepped nature of the surfaces is clearly visible in low angle SEM micrographs of unincorporated whiskers [13]. The dimensions of the 'notches' formed in the zig-zag sequence of the stacked polytypes correlate with distances between the planar faults intersecting the whisker surface. Because of the microfaceting, the whisker surface is rough on the scale of a few inter-

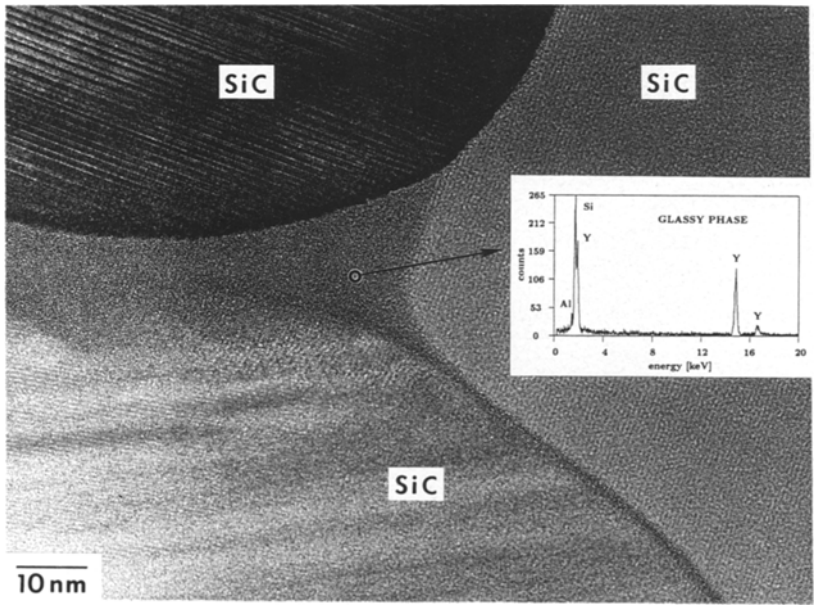

Figure 7 Amorphous triple-grain junction from Si_3N_4 base composite adjacent to three β-SiC whiskers in different contrast conditions (400 kV). Note enrichment of yttrium in non-crystalline phase, as indicated by the EDS spectrum inset.

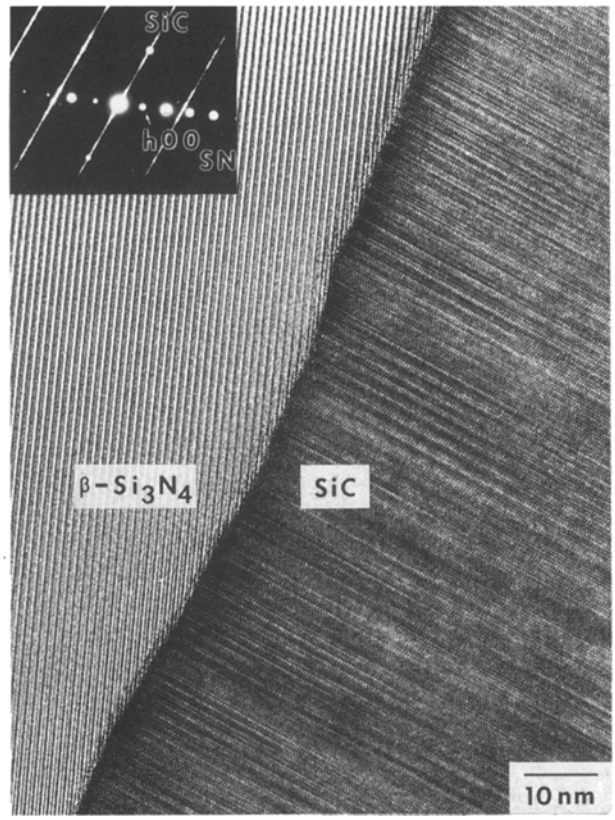

Figure 8 HREM image (400 kV) of β-SiC/β-Si_3N_4 boundary taken from the boxed region of Fig. 3. The orientation of β-Si_3N_4 is close to [0 0 1], the beam direction in the whisker is close to [1 1 0] (see diffraction pattern inset).

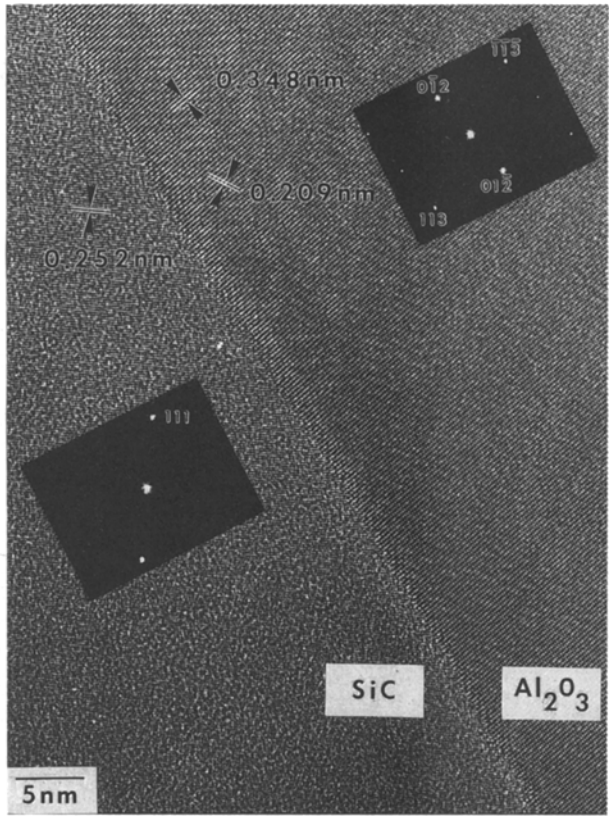

Figure 9 HREM image (400 kV) from a β-SiC/α-Al_2O_3 interface oriented edge-on. Beam directions are close to [1 1 0] in β-SiC and parallel to [5–$\bar{2}$–$\bar{1}$] in corundum, respectively (see optical diffractograms). For corresponding low-magnification image, see Fig. 5.

atomic spacings, and the whisker surface area is significantly increased, along with the corresponding interfacial area for bonding to a fine-grained ceramic host matrix. The stepped surface structure is a characteristic feature of VLS-grown β-SiC whiskers that has been established for whiskers from different sources [13, 14].

In dense Si_3N_4, to which sintering aids were added during processing, a non-crystalline phase is generally dispersed throughout the microstructure, at triple grain junctions and in grain boundaries. It may also be a continuous intergranular thin film separating hot matrix grains. As a consequence, surfaces in the corresponding composite SiC whiskers were wetted by the liquid phase in areas of high secondary phase concentration (see Fig. 3). Fig. 7 shows a triple grain pocket of non-crystalline phase adjacent to three SiC-whiskers. EDS microanalysis revealed yttrium enrichment relative to silicon in this phase. According to phase relationships in the system Y_2O_3–Al_2O_3–Si_3N_4, for the conditions used for our composite fabrication, a substantial nitrogen solubility in the non-crystalline phase was to be expected. However, ELS did not resolve an N–K edge in this particular glass pocket either because it was too thick, or because nitrogen was not present. In thinner foils of this material nitrogen was often observed by ELS in some, but not all glass pockets: that is, nitrogen was not homogeneously distributed. No corrosive attack of the oxynitride liquid on whisker surfaces was observed. However for Si_3N_4 base composites processed at a considerably higher temperature (1850° C), attack has been reported, giving rise to notches about 10 nm deep into SiC whiskers [14].

The extension of the glassy grain-boundary phases from triple-grain junctions along the associated grain boundaries in ceramics has been demonstrated elsewhere by dark-field imaging [15]. A major observation of this study was the existence of entirely crystalline β-SiC/crystalline matrix interfaces. An HREM image of an β-SiC/β-Si_3N_4 boundary oriented edge-on (corresponding to the boxed area in Fig. 2) is shown in Fig. 8. A few whisker/matrix interfacial boundaries that contained a glassy phase were observed in this material, but most did not. Moreover, the glassy phase was not continuous in the boundaries. The HREM image also shows a lack of interfacial reactions, although the interface is not atomically smooth. The local roughness is obviously related to the stepped whisker surface. Contrast variations observed at the interface for a given defocus are believed to have resulted from slight deviations of the correct edge-on orientation of the boundary with respect to the electron beam, or to local thickness fluctuations of the foil due to preferential thinning at the interface. Local thickness variations were verified by small-probe low-loss ELS as a function of position near the interfaces from composites of this study and similar materials [16].

Boundaries between Al_2O_3 and β-SiC whiskers are shown in Figs 9 and 10. There is no evidence for an amorphous phase in the edge-on interface shown in Fig. 9. The fringes of each constituent end abruptly at the interface, although some nearly atomic scale

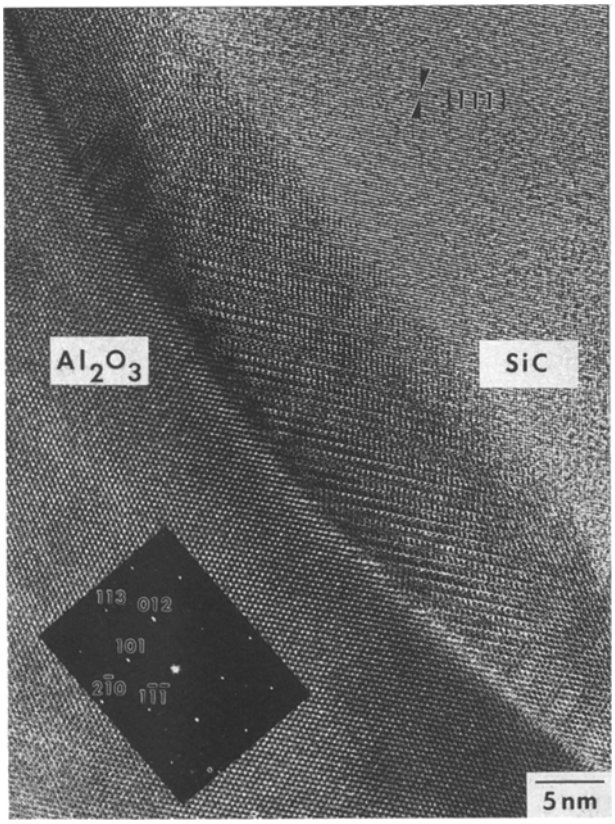

Figure 10 Inclined boundary (400 kV) revealing Moiré contrast between α-Al_2O_3 (beam direction parallel [1–$\bar{2}$–$\bar{1}$], see optical diffractogram) and β-SiC (orientation close to [1 1 0]).

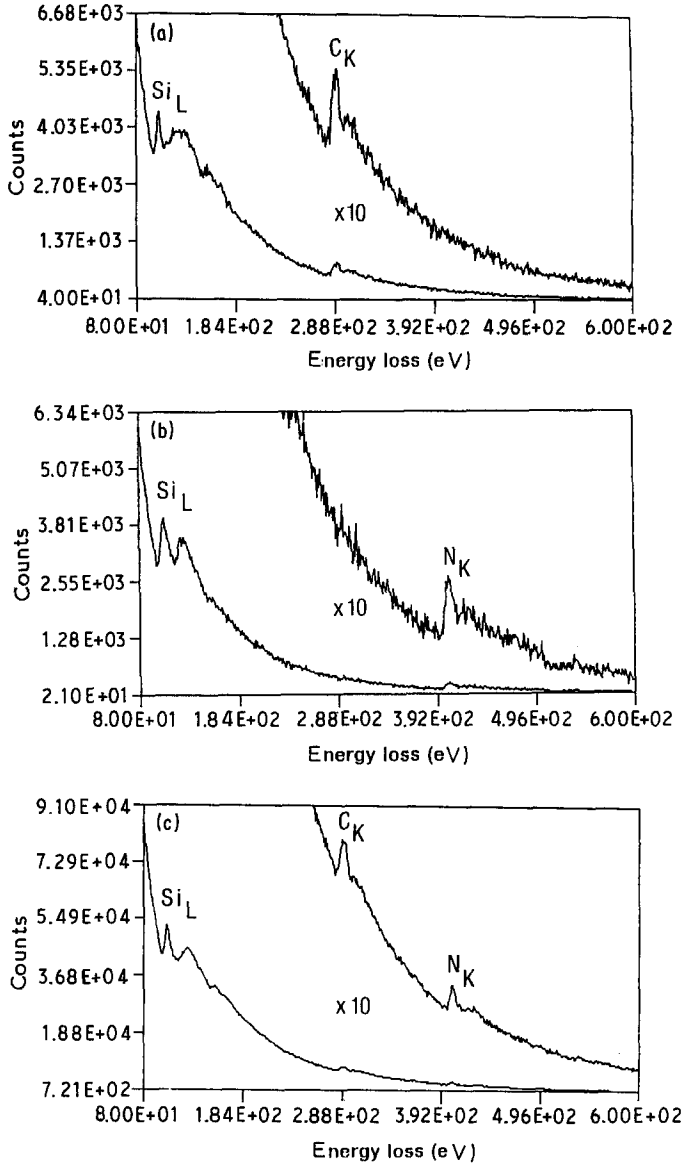

Figure 11 ELS spectra collected at 100 kV using serial detection with a 5 nm FEG TEM probe from interfacial constituent phases and the boundary in the Si_3N_4 base composite (a) from the whisker (5 nm from interface); (b) from the matrix (5 nm from interface); (c) 5 nm probe centred on interface (interface is aligned with incident beam direction).

roughness is evident, as noted above for the other composite. An inclined whisker/Al_2O_3 boundary is shown in Fig. 10. Regular Moiré contrast is visible in the entire overlap region with no localized disturbances due to hemispherical cap crystalline reaction zones between Al_2O_3 and SiC. Whisker/matrix interfaces in this material have also been examined using small-probe convergent-beam microdiffraction and energy-loss spectroscopy, but no eividence was found for segregation, amorphous phases or crystalline reaction zones.

A more extensive examination of some of the Si_3N_4/SiC interfaces was conducted using ELS. This material was considered more likely to exhibit possible light-element segregation (oxygen, carbon or nitrogen) or amorphous phases at the whisker/matrix interfaces, because a sintering aid was added during fabrication, in addition to the light-element enrichment on the surfaces of the as-received whiskers. The results, as shown in Fig. 11, did not provide evidence for amorphous phases or segregation. Note that there are slight indications of a residual oxygen peak at 531 eV in Figs 11b and c. But, since this occurred in both matrix Si_3N_4 and the interface spectra, it cannot be ascribed to interfacial segregation. No reaction products such as spinel, mullite, or aluminium- and silicon-bearing carbides or oxycarbides were identified at any whisker/matrix interfaces.

In both composites SiC appears primarily to be bonded directly to the matrix ceramic. The absence of distinct chemical reaction layers (that is, third phases) for this class of SiC whisker-reinforced ceramic composite is in accord with previous investigations [14, 15].

One of the few amorphous regions observed in the Al_2O_3/SiC composite is shown in Fig. 12. Note that this region occurred at an Al_2O_3 matrix triple-grain junction and not at a SiC/Al_2O_3 interface. The region is multiphase and consists of graphite fibres distributed in an amorphous matrix. Energy-loss spectroscopy showed that the amorphous matrix contained oxygen, and X-ray spectroscopy showed the presence of aluminium, silicon and a small amount of calcium, but no magnesium was detected. The graphite is believed to have either (i) formed after condensation of a carbon-rich vapour phase accidentally trapped in a glassy-phase pocket, or (ii) nucleated from an oxycarbide liquid phase. Homeny and co-workers [17] showed recently that carbon solubility reaches about 2.5 wt % at 1800° C in the system Al–Si–Mg–O–C. In either case the source of carbon was probably related to excess carbon on the surface

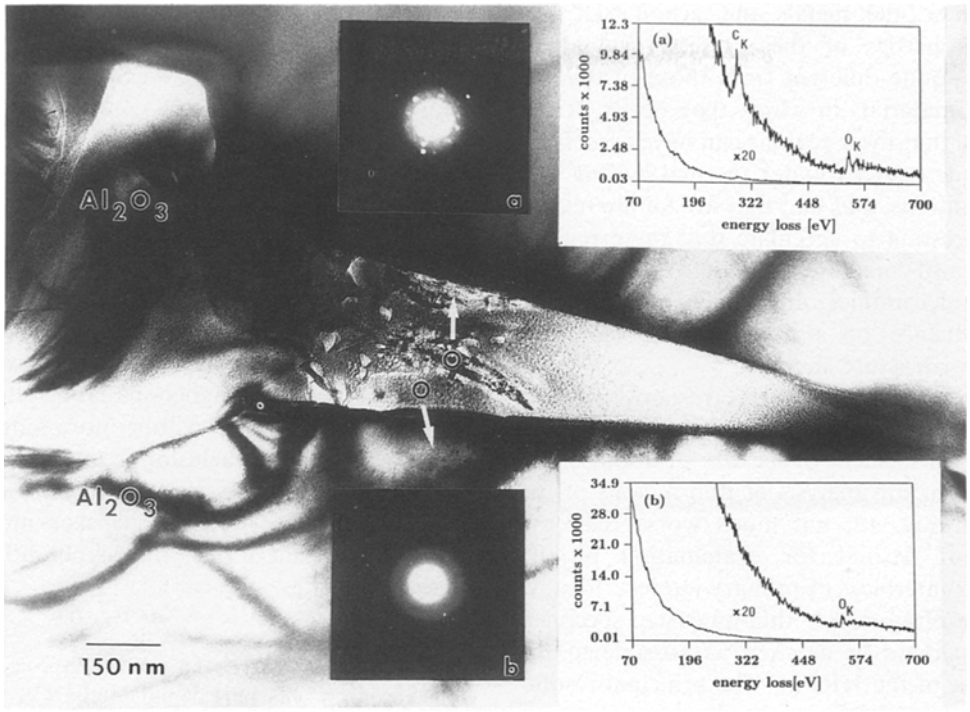

Figure 12 Amorphous triple-grain junction in Al_2O_3 base composite showing precipitation of graphite filaments, as confirmed by CBED and ELS, inside non-crystalline phase. ELS spectra of the graphite and the glassy phase originate from probe locations indicated. EDS spectra not shown.

of whiskers, although simple impurity pick-up during processing may have contributed.

4. Discussion

To understand the effect of interfacial properties on SiC whisker-toughening mechanisms it is of fundamental importance to establish whether whisker surfaces in the consolidated composite are continuously wetted by thin amorphous films. For dense monolithic Si_3N_4 matrices, the continuous character of the silicon oxynitride liquid along large-angle grain boundaries, at least at high temperatures, is well established by TEM [18–20]. Thus, given the oxygen-rich surface chemistry of as-received SiC whiskers, the lack of a continuous phase at crystalline whisker/matrix boundaries is somewhat surprising, particularly in the Si_3N_4 base composite, to which oxide sintering aids were also added. However, similar findings in a MgO-doped Si_3N_4 matrix composite material were reported by Backhaus-Ricoult and co-workers [21] from ELS microspectroscopy performed at crystalline SiC/Si_3N_4 interfaces. Recent HREM studies of nanoscale β-SiC inclusions dispersed intergranularly into Al_2O_3 as well as in Si_3N_4 matrix grains also did not indicate interfacial reaction layers or amorphous films at the boundaries [22]. The fact that high-temperature creep performance has been reported to be unaffected by SiC whisker incorporation into Al_2O_3 [23] as well as in Si_3N_4 base composites [21] may be further indirect evidence for the direct bonding of whiskers to matrix at such crystalline interfaces.

Regarding the substantial amounts of excess carbon and silicon established for the as-received whisker surfaces, the removal of such whisker surface constituents via CO or SiO vapour-phase reactions at a stage of remaining porosity during composite densification appears reasonable. If the initial surface was indeed silica-rich, reactions like $SiC + 2SiO_2 \rightarrow 3SiO\uparrow + CO\uparrow$ and/or $SiO_2 + 3C \rightarrow SiO\uparrow + 2C + CO\uparrow$ appear to be the most likely reaction paths for locally deoxidizing the whisker circumference. Secondary SiC deposition, according to the Acheson-process-related reaction $SiO_2 + 3C \rightarrow SiC + 2CO\uparrow$, was not observed. Because the rates of the proposed reactions are depressed by gas species added to the system, SiO and/or CO generation may actually be more efficient in the vacuum-processed Al_2O_3/SiC material than in the Si_3N_4 base composite, which was hot-pressed in argon atmosphere. However, weight-loss variations could not be monitored continuously during composite processing, so these mechanisms only furnish plausible qualitative explanations for changes in whisker-surface composition.

The multiphase amorphous regions observed at a few α-Al_2O_3 triple junctions in the Al_2O_3/SiC composite are unusual. These were in fact rather large, with the largest maximum dimension often being about one μm. It is worth noting that similar regions have been observed in quite dissimilar structural ceramics, such as sintered α-SiC [24, 25] and in liquid phase sintered SiC [26]. The starting materials and processing methods for the various structural ceramics in which these particular similar multiphase regions occur are all different, so their formation mechanisms must differ to an unknown extent. However, their common morphological features are striking – they all contain crystalline graphite fibres in an amorphous matrix that always contains appreciable oxygen. The differences among the various ceramics are primarily the relative amount of graphite in the amorphous material, and the metallic constituents of the amorphous matrix, which may be aluminium,

silicon, yttrium or other metals, and carbon itself. The mechanical properties of these regions would be expected to be quite different from those of the primary ceramic materials in which they occur. It has been suggested that these regions can have associated cavities and microcracks under thermal cycling and creep-test conditions, and that they are failure related [27]. It is interesting to speculate that these regions may be a class of 'macrodefects' that may occur in many structural ceramics, and which may have an important influence on the often observed wide scatter-band for fracture strength.

The electron-energy-loss spectroscopy results presented here merit some comment. These were obtained with an incident probe size of about 5 nm, which is sufficient for analysis of thin regions of the type shown in Fig. 12, but much worse than the resolution limit desired for examination of the whisker/matrix interfaces of primary interest. Ideally, the spatial resolution for thin-interface specimen microanalysis should be as close as possible to the resolution limit of the HREM. The principal resolution limits for serial ELS microanalysis are specimen and probe drift during the length of the time required to obtain a serial spectrum, even with the use of a field-emission electron source The total time usually amounts to about 100 sec (1000 channels and 100 msec dwell per channel) for a spectrum with sufficient counts for quantitative and fine-structure analysis, although better resolution can be obtained if spectrum quality is of less concern. A parallel ELS collection system now in the final stages of development will reduce the required collection time by a factor between 500 and 1000, and greatly improve spatial resolution; the limiting factors will then become current distribution in the probe, and elemental distribution in the irradiated volume. The resulting spectrum will represent a convolution of these factors. We have presented preliminary results of probe-current distribution for the analytical microscope used here [28] and estimated the best attainable spatial resolution to be between 1 and 2 nm with the new system [29]. When the elements of interest are most concentrated at the interface, it is obviously desirable to use the smallest probe possible, consistent with probe current and specimen radiation damage limits. A spatial resolution limit between 1 and 2 nm can probably be used for quantitative analysis of most thin intergranular films so far reported, or for non-equilibrium segregation, but measurements of equilibrium segregation will be more difficult. The interfaces discussed here will be re-examined with the parallel detection spectroscopy system, with particular emphasis on whisker/matrix interface segregation.

5. Conclusions

The interfaces between β-SiC whiskers and adjacent crystalline matrix grains of either β-Si_3N_4 or α-Al_2O_3 in the composites examined did not in general contain thin amorphous films; the whiskers were directly bonded to the matrix crystals in both materials over most of the interface area examined. Some of these interfaces (the minority) contained glassy phase, with more in the Si_3N_4 matrix composite than in the Al_2O_3 matrix composite; this correlates directly with sintering aid additives present in the Si_3N_4 composite, which were absent from the Al_2O_3 composite. We conclude that amorphous thin films are not generally present in whisker/matrix interfaces in these composites, and the probability of their presence depends strongly on the amount of sintering aid added during processing.

Light-element segregation at fully crystalline whisker/matrix interfaces (based on HREM observations) was investigated by ELS experiments at 5 nm spatial resolution, but none was detected. This result is valid, but it is noted that higher-spatial-resolution experiments to be conducted will be more sensitive to segregation, and this conclusion is therefore tentative.

No crystalline reaction zones were observed to have been formed between the SiC whiskers and the matrix crystals as a result of the synthesis conditions used for these composites.

Acknowledgements

This research was performed in the Center for Solid State Science, High Resolution Electron Microscopy Facility, while W. Braue was a visiting scientist. The support of the United States Department of Energy (Grant DE-FG02-87ER45305) and from Deutsche Forschungsgemeinschaft (DFG), FRG and the Center for Solid State Science is gratefully acknowledged. Si_3N_4 and Al_2O_3 composites provided for this study were processed by G. Woetting, now with CFI, Roedenthal, FRG, and R. Wagner, DFVLR, Cologne, FRG, respectively. Helpful comments were contributed by R. Cutler, Ceramatec, Inc., Salt Lake City, Utah, USA; K. Niihara, The National Defense Academy, Yokosuka, Japan; and A. Hoelscher, DFVLR, Cologne, FRG.

References

1. G. C. WEI and P. F. BECHER, *Amer. Ceram. Soc. Bull.* **64** (1985) 298.
2. P. D. SHALEK *et al.*, *ibid.* **65** (1986) 351.
3. S. T. BULJAN, J. G. BALDONI and M. L. HUCKABEE, *ibid.* **66** (1987) 347.
4. M. R. RUEHLE, B. O. DALGLEISH and A. G. EVANS, *Scripta Met.* **21** (1987) 681.
5. J. HOMENY and W. L. VAUGHN, *MRS Bull.* **7** Oct/Nov (1987) 66.
6. P. ANGELINI, W. MADER and P. F. BECHER, *Mater. Res. Soc. Symp. Proc.* **78** (1987) 241.
7. A. HOELSCHER, W. BRAUE and G. ZIEGLER, in preparation.
8. J. V. MILEWSKI *et al.*, *J. Mater. Sci.* **20** (1985) 1160.
9. N. K. SHARMA, W. S. WILLIAMS and A. ZANGVIL, *J. Amer. Ceram. Soc.* **62** (1984) 715.
10. K. H. JACK, *J. Mater. Sci.* **11** (1976) 1135.
11. S. SHINOZAKI and K. R. KINSMAN, *Acta Metall.* **26** (1978) 769.
12. S. R. NUTT, *J. Amer. Ceram. Soc.* **71** (1988) 149.
13. L. F. ALLARD, P. PENDLETON and J. S. BRINEN, in Proceedings of the 44th Annual Meeting of the Electron Microscopy Society of America, Albuquerque, New Mexico, USA, August 10–15, 1986, edited by G. W. Bailey (San Francisco Press, San Francisco, 1986) p. 472.
14. S. R. NUTT and D. J. PHILIPS, in Symposium on Interfaces in Metal–Matrix Composites, Annual Meeting of the Metallurgical Society, New Orleans, Louisiana, March 1986, edited by A. K. Dhingra and S. G. Fishman, p. 111.

15. V. K. SARIN and M. RUEHLE, *Composites* **18** (1987) 129.
16. P. R. T. JANG and R. W. CARPENTER, in Proceedings of the 44th Annual Metting of the Electron Microscopy Society of America, Albuquerque, New Mexico, USA, August 10–15, 1986, edited by G. W. Bailey, (San Francisco Press, San Francisco, 1986) p. 718.
17. J. HOMENY, G. G. NELSON and S. H. RISBUD, *J. Amer. Ceram. Soc.* **71** (1988) 386.
18. D. R. CLARKE, *Ultramicroscopy* **4** (1979) 33.
19. L. K. V. LOU, T. E. MITCHELL and A. H. HEUER, *J. Amer. Ceram. Soc.* **61** (1978) 462.
20. H. SCHMIDT and M. RUEHLE, *J. Mater. Sci.* **19** (1984) 615.
21. M. BACKHAUS-RICOULT, J. CASTAING and J. L. ROUTBORT, *Rev. Phys. Appl.* **23** (1988) 239.
22. K. NIIHARA *et al.*, in Proceedings of the 3rd International Symposium on Ceramic Materials and Components for Engineers, Las Vegas, Nevada, November 1988, pp. 919–926.
23. J. R. PORTER, F. F. LANGE and A. H. CHOSKI, *Mater. Res. Soc. Symp. Proc.* **78** (1987) 289.
24. W. M. SKIFF and R. W. CARPENTER, in Proceedings of the 40th Annual Metting of the Electron Microscopy Society of America, Washington, D.C., USA, August 9–13, 1982, edited by G. W. Bailey (San Francisco Press, San Francisco, 1982) p. 564.
25. W. BRAUE and R. W. CARPENTER, *J. Mater. Sci.* **25** (1990) 2943.
26. R. W. CARPENTER, W. BRAUE and R. A. CUTLER, in Proceeding of the 45th Annual Meeting of the Electron Microscopy Society of America, Baltimore, Maryland, USA, August 2–7, 1987, edited by G. W. Bailey (San Francisco Press, San Francisco, 1987) p. 306.
27. N. J. TIGHE, K. A. HARDMAN-RHYNE and Y. N. LU, in Proceedings of the 9th Annual Conference on Composites and Advanced Materials, Cocoa Beach, Florida, USA, January 20–23, 1985 (American Ceramic Society, 1985) p. 835.
28. J. K. WEISS and R. W. CARPENTER, in Proceedings of the 46th Annual Meeting of the Electron Microscopy Society of America, Milwaukee, Wisconsin, USA, August 7–12, 1988, edited by G. W. Bailey (San Francisco Press, San Francisco, 1988) p. 510.
29. R. W. CARPENTER, *Mater. Sci. Engng* **A107** (1989) 207.

Received 15 March 1989
and accepted 20 June 1989